Zeitschrift: IABSE reports = Rapports AIPC = IVBH Berichte
Band: 67 (1993)

Artikel: Finite element prediction of a destructive field test of a bridge
Autor: Borst, René de / Veen, Cor van der / Blaauwendraad, Johan
DOI: https://doi.org/10.5169/seals-51376

Finite Element Prediction of a Destructive Field Test of a Bridge

Prédiction de la charge de rupture d'un pont au moyen des éléments finis

Vorausberechnung einer Betonbrücke im zerstörenden Feldversuch mittels Finiter Elemente

René de BORST
Prof. Dr.
Delft Univ. of Technology
Delft, The Netherlands

Cor van der VEEN
Dr. Eng.
Delft Univ. of Technology
Delft, The Netherlands

Johan BLAAUWENDRAAD
Prof. Dr.
Delft Univ. of Technology
Delft, The Netherlands

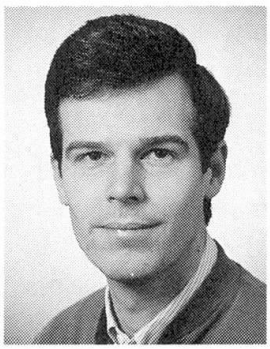

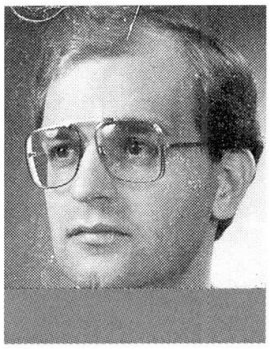

René de Borst, born in 1958, received his Ir.degree in civil engineering in 1982 and his Dr. degree in 1986, both from Delft University of Technology. He is professor of computational mechanics at the Faculty of Civil Engineering of Delft University of Technology since 1988 and senior research fellow of the Netherlands Organization for Applied Scientific Research (TNO) since 1990.

Cor van der Veen, born 1953, received his Ir. degree in civil engineering in 1982 and his Dr. degree in 1990, both from Delft University of Techbology. He is currently a senior reseacher in bridge design and computational modelling at the Faculty of Civil Engineering of Delft University of Technology.

Johan Blaauwendraad, born 1940, received his Ir. degree in civil engineering in 1962 and his Dr. degree in 1973, both from Delft University of Technology. He joined the Netherlands Organization for Applied Scientific Research (TNO) in 1964 and Rijkswaterstaat in 1971. He is professor of civil engineering at Delft University of Technology since 1979.

SUMMARY

Nonlinear finite element analyses have been carried out to predict the load-carrying capacity of a forty-year old, three-span skewed-slab bridge. By sensitivity studies the uncertainty in the boundary conditions and the possible impact of the existing damage on the failure load have been assessed. Proper lower and upper-bound finite element solutions have been obtained in this way. The numerically predicted failure load appeared to underestimate the experimental collapse load by less than 10%.

RÉSUMÉ

Une analyse non linéaire par éléments finis a été utilisée pour prédire la résistance d'un pont biais à trois travées, construit il y a 40 ans. L'influence des conditions aux limites et des dommages au pont ont été pris en compte par une étude de sensibilité, et les bornes inférieures et supérieures de la résistance du pont ont ainsi été calculées. La prédiction de la charge de rupture a été trouvée légèrement inférieure (10%), à la charge réelle constatée expérimentalement.

ZUSAMMENFASSUNG

Die Traglast einer vierzig Jahre alten, dreifeldrigen gekrümmten Plattenbrücke wurde aufgrund einer nichtlinearen Finite-Element-Studie vorhergesagt. Der Streubereich der Randbedingungen und der Einfluss von Vorschädigungen auf die Traglast wurde im Rahmen einer Parameterstudie abgeschätzt. Auf diese Weise ergaben sich obere und untere Schrankenlösungen. Die vorausberechnete Traglast lag mit weniger als 10 % auf der sicheren Seite der experimentell bestimmten Traglast.

1. INTRODUCTION

After a thirty-year development the finite element method has become a powerful tool for analysing structural behaviour. By now, deflections and stresses under service load levels can be predicted within a tolerance that is narrower than the scatter in material properties and the uncertainty due the boundary conditions, which are often not known precisely. Unfortunately, this statement cannot always be carried over to the failure regime. Especially for concrete and masonry structures there is still a lack of robust computational tools which can provide *reliable predictions* of the structural performance in the failure and the post-failure regime. Predictions of the load-carrying capacity that exceed the experimental failure load by a factor two are not uncommon, and at some instances a proper failure load cannot be obtained at all. Publications in which the failure load of such structures is computed accurately mostly relate to *postdictions* rather than to *predictions.*

In this contribution we shall describe *predictive* finite element analyses of a three-span, skewed-slab bridge, which has been tested to failure afterwards by a team of the University of Cincinnati and Wiss, Janney and Elstner [1]. The bridge was built in 1953 and was located on Route 222 in Clermont County, Ohio. Visual inspection prior to the analyses and the testing revealed that the concrete had experienced extensive deterioration and that there was corrosion in some bars.

In the non-linear finite element analyses concrete cracking and plastification of reinforcement and concrete in compression have been taken into account. The sensitivity of the model to the various material parameters has been investigated by means of parametric studies. In this way the effect of the existing damage on the load-carrying capacity could be quantified. Furthermore, the possible impact of the assumed boundary conditions on the predicted failure load was assessed.

2. DESCRIPTION OF THE BRIDGE AND THE FIELD TEST

The bridge which has been analysed and tested is a three-span, skewed-slab bridge and is shown in Figure 1, see also Reference [1], which provides the necessary details on the lay-out of the reinforcement as well. Inspection prior to the analyses and the testing revealed that severe damage had occurred, especially near the sides of the bridge [1], while the driving lanes were in a reasonable condition. In the areas of visible damage of the concrete the reinforcing bars had corroded severely. The visual inspection was hampered by the existing asphaltic overlay, which was removed only shortly before the final destructive testing.

To obtain a better judgement of the concrete properties cores were drilled at several places. The concrete test specimens were then subjected to uniaxial compression tests which resulted in values for the mass density ρ and for the uniaxial compressive strength f_c which ranged from 2450 kg/m^3 to 2470 kg/m^3 and from 49 MPa to 56 MPa respectively. The value for Young's modulus E appeared to be around 33000 MPa. As will be detailed below, in the analyses the possible effect on the remaining structural capacity of the observed poor quality of the concrete was modelled by adopting artificially low values for Young's modulus and for the uniaxial compressive strength. Properties for the reinforcing steel could be derived from uniaxial tension tests on rebars, see for instance Figure 2 [1].

Prior to the final destruction test modal tests were carried out in order to obtain data on the boundary conditions which would have to be applied in the analyses. In contrast to the final destruction test the modal test were conducted with the asphaltic layer still in place, and resulted in a lowest eigenfrequency of approximately 8.3 Hz [1].

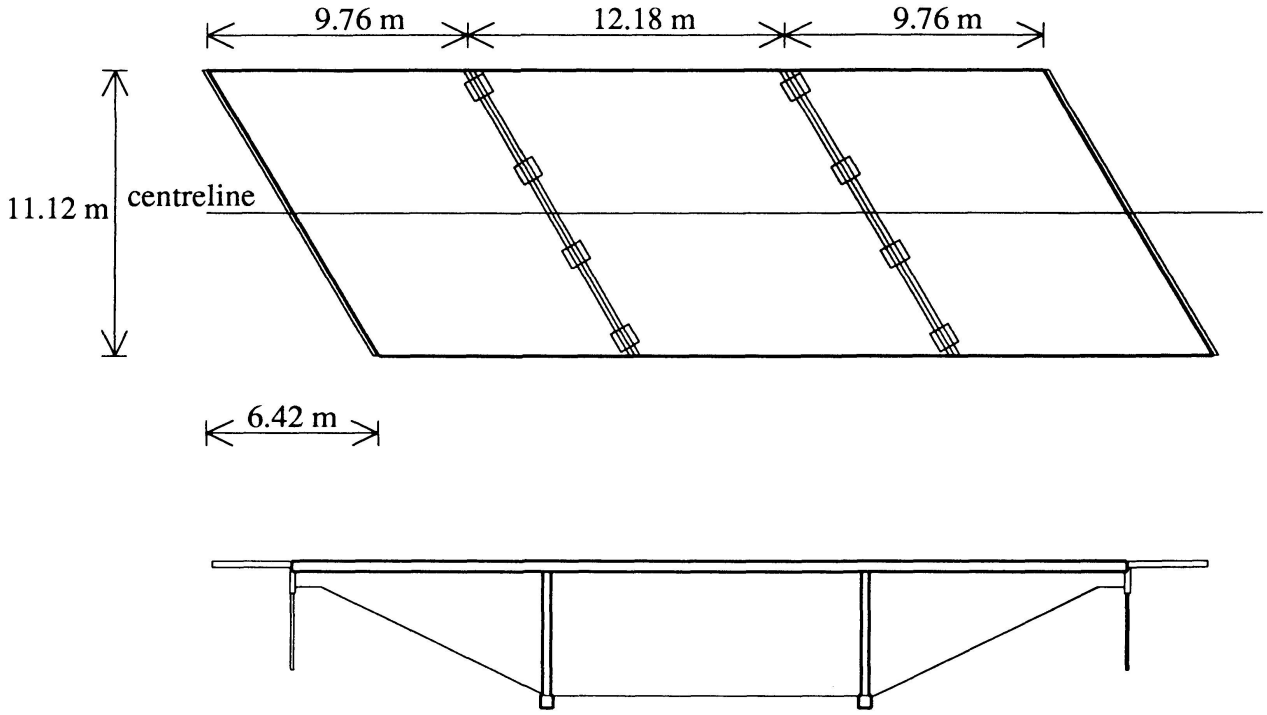

Figure 1 Plan view and side view of the bridge.

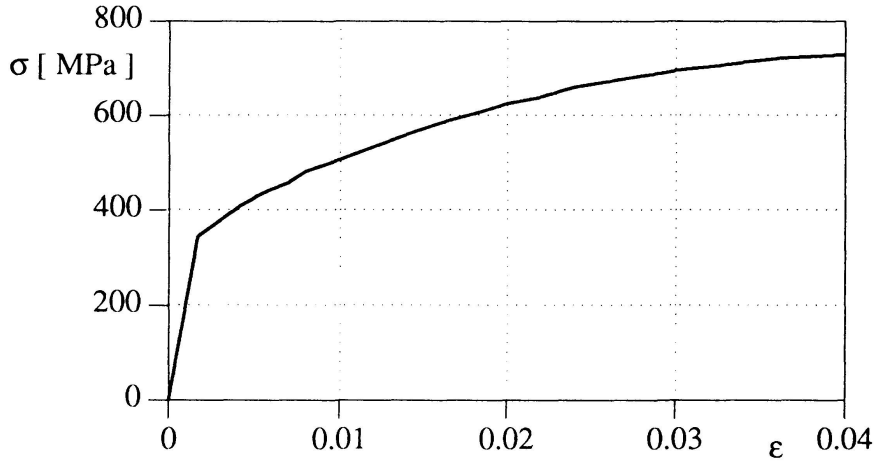

Figure 2 Experimentally obtained stress-strain curve of a tension test on a reinforcing bar.

The actual destructive tests were carried by pulling down two concrete blocks of 0.6 m by 1.8 m, which were placed on the bridge deck in order to distribute the forces exerted by servo-controlled hydraulic actuators. On each block two of such actuators were placed. Rock anchors were attached to the actuators to provide the reaction force that was needed to load the bridge. The total load at which failure occurred was 3.24 MN. In the remainder of this article we shall always refer to the load that was exerted on one of the blocks only, so that collapse occurs at a load level of 1.62 MN.

3. PREDICTIVE ANALYSES

3.1 Analytical yield line analyses

When the authors started their non-linear finite element analyses a rough estimate of the final collapse load had been obtained by the investigators at the University of Cincinnati. They had carried out yield line analyses assuming four different yield line patterns [1]. For the boundary conditions that have been used in the Delft finite element analyses and for the material data used in the reference finite element calculation (see below), the collapse load per loading block varied from 1.5 MN to 2.67 MN [1].

3.2 Discretization and loading configuration

The finite element mesh that was adopted in the analyses which have been carried out with the DIANA finite element package is shown in Figure 3. It consists of 144 eight-noded degenerated plate/shell elements with a 2×2 Gauss integration in the plane and a nine-point Simpson integration through the depth. Reinforcement was modelled using an embedded approach, that is the interpolation functions of the concrete were used also for the reinforcement. The reinforcement grid has its own integration stations, which do not have to coincide with the layers of the plate/shell element. The discretization of Figure 3 was considered sufficiently refined for the expected bending-type failure. Analyses with different meshes should have been tried to verify this, but, because of time restrictions - the analyses had to be completed before the actual bridge testing - this has not been done.

The loading blocks have been modelled as two line loads which were each placed at the edges of two elements, see Figure 3. Linear dependence relations have been supplied to ensure that all nodes beneath a line load had the same vertical displacements.

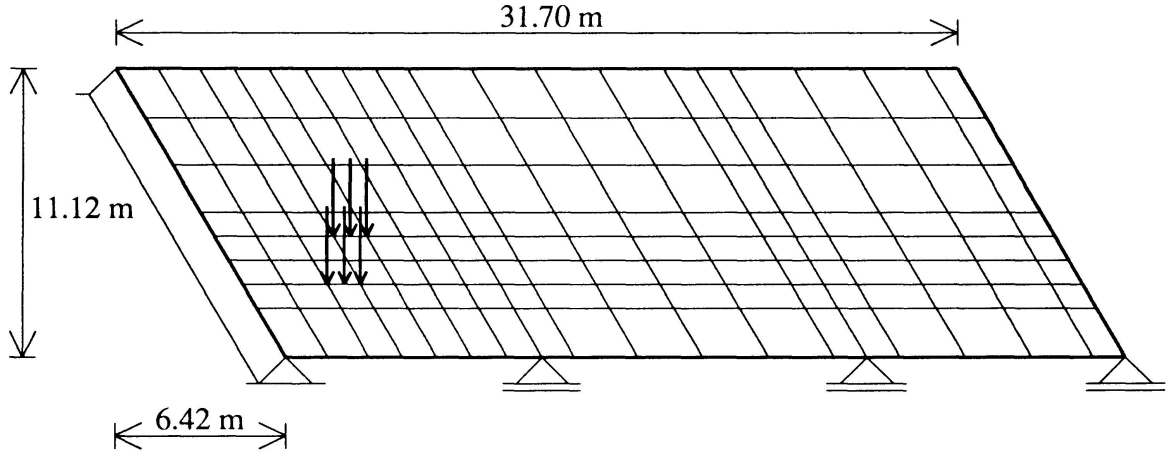

Figure 3 Finite element model for the Delft FE analysis of the bridge and position of the loads.

3.3 The numerical solution procedure

All load-deflection curves that will be presented in the remainder of this article correspond to converged solutions in which a force norm of 10^{-2} was satisfied after 4-5 equilibrium iterations with a Modified Newton-Raphson scheme, in which the stiffness matrix was set up at the beginning of each loading step. For the plasticity models this matrix was the tangent stiffness matrix and for the cracking model the secant stiffness matrix was substituted. At the points were

the calculations have been terminated further analysis was always possible. Rather large steps have been taken, approximately fifty for the upper bound solution and only five for the lower bound solution. The upper bound solution calculations in which the step size was halved showed that for this structure even the coarse loading steps were fine enough.

3.4 Assessment of the boundary conditions

The piers have not been modelled in the predictive analyses, because they have no influence on the final collapse load or the failure pattern. However, there is some influence on the load-deflection pattern, not only because of the neglected axial stiffness of the piers, but also because the piers act as rotational springs on the bridge deck. From a hand calculation it appeared that the maximum axial shortening of the piers would be approximately 0.1 mm, which is negligible. The rotational stiffness of the piers was not taken into account either. This simplification will be justified below.

A most important issue when modelling an existing structure is the interaction of the structure with the environment. At the abutments as well as at the piers we have the question whether the most appropriate boundary condition would be a clamped support, a hinged support, or a roller support. The question of clamped support *vs* hinged support can be partly resolved by carrying out eigenvalue analyses and comparing the numerical results with the lowest eigenfrequency that comes out of the modal test ($\simeq$ 8.3 Hz). In the finite element analyses with the mesh of Figure 3 the mass density of the concrete was taken as ρ = 2370 kg/m^3 and Young's modulus E and Poisson's ratio were assumed as 24800 MPa and 0.2 respectively. The reduced value for Young's modulus was adopted to model the observed deterioration of the concrete. In the first analyses all supports were assumed to be hinged. When the influence of the asphaltic concrete cover was neglected an eigenfrequency of 7.43 Hz was computed, whilst the slightly lower value of 6.76 Hz was found for the analysis in which the asphaltic concrete cover was included. These values are much closer to the experimentally determined eigenfrequency than the value of 22.69 Hz that was obtained for the case with clamped ends and hinged supports at the piers. This indicates that (i) the supports at the abutments are not clamped and (ii) neglecting the bending stiffness of the piers is reasonable. However, the issue of hinged *vs* roller supports cannot be answered by modal analyses and will be investigated below.

3.5 Model parameters for non-linear finite element analysis

In the non-linear analyses the following data have been used. For the reinforcement an elastic-plastic model was utilized with a Young's modulus E_s = 200000 MPa, an initial yield strength σ_{sy} = 345 MPa and a hardening modulus h = 7000 MPa, which is in agreement with the experimentally supplied data. The inelastic behaviour of concrete in tension has been modelled by the multiple fixed crack model of de Borst and Nauta [2] and Rots [5]. The shear retention factor β was set equal to 0.2 in all analyses. For the expected type of bending failure a variation of β hardly has any impact on the results.

To account for the stiffness of the concrete between the smeared-out cracks a tension-stiffening model was adopted with a linear softening branch and an ultimate strain at which the residual load-carrying capacity is exhausted $\varepsilon_u = {}^1/_2 f_{sy}/E_s$. The factor ${}^1/_2$ has been introduced because previous experience has shown that this generally leads to a better prediction of the structural behaviour [4] and because a hand calculation for a rectangular cross section showed that taking $\varepsilon_u = f_{sy}/E_s$ would result in a moment at which the steel starts yielding, M_{sy}, that is larger than the moment at which collapse ultimately occurs (M_u).

The concrete stresses in biaxial compression were limited by a Drucker-Prager yield contour,

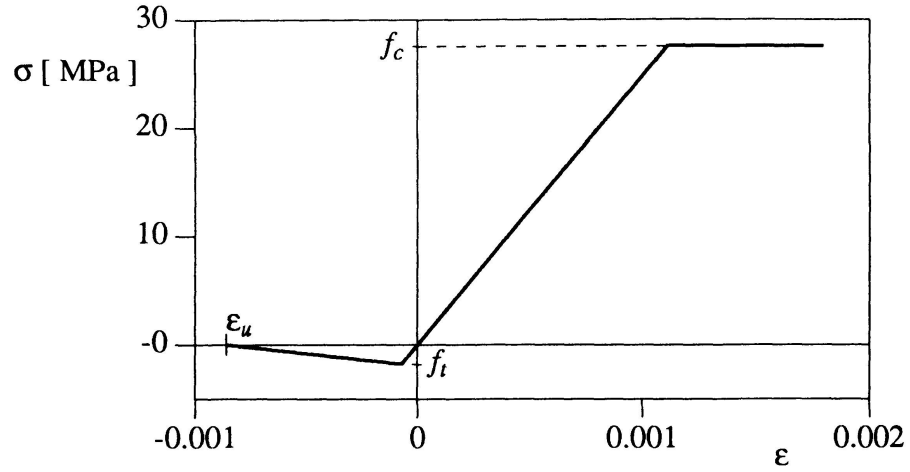

Figure 4 Uniaxial response of concrete for the reference set of model parameters.

which was fitted such that the pure biaxial compressive strength f_{bc} equals 1.16 times the uniaxial compressive strength f_c. Perfectly plastic behaviour was assumed thereafter, because any introduction of softening in compression would result in an extreme mesh sensitivity, which cannot yet be modelled properly. The uniaxial compressive strength f_c itself was set equal to 27.5 MPa. This is a relatively low value, and was adopted to account for observed damage in the concrete. The tensile strength was initially set equal to f_t = 3.2 MPa, which is the value that had been suggested by investigators of the University of Cincinnati [1], but later the value f_t = 1.8 MPa has been used which follows from applying $f_t = 0.75 \cdot (1 + f_c/20)$, which formula is used in the Dutch Codes of Practice. In parameter studies it later appeared that the tensile strength affects the load-deflection curve only in the first stages of cracking. The uniaxial stress-strain curve that results from the adopted set of reference parameters is shown in Figure 4.

3.6 Numerical results

When carrying out non-linear finite element analyses it is sensible to first concentrate on the most important causes of the non-linear structural behaviour, cf. the almost pedagogic treatise of Meyer [3]. For 90% of all reinforced concrete structures cracking and yielding of the reinforcement are the dominant non-linear phenomena which govern the structural response. Therefore, firstly analyses were carried out in which concrete plasticity was not taken into account. These analyses were carried out under arc-length control with a novel and very robust method for estimating the load increment in a step [6]. The results are the upper and lower curves of Figure 5. In these figure half the total load has been plotted against the deflection of the outermost loading block. The upper curve was obtained under the assumption that all supports (at the abutments and at the piers) were hinges, while the lowermost curve was obtained assuming that all supports were rollers except for one of the abutments.

We observe that this variation in boundary conditions has a tremendous impact on the structural response of the bridge. This phenomenon can be explained as follows. In the latter case (the lower-bound solution) cracks due to the bending moments penetrate deep into depth of the slab which causes large horizontal strains in the midplane of the slab. As a consequence an axial elongation of the midplane occurs. On the other hand, this elongation is entirely prevented in case of hinges at all supports. This means that additional in-plane forces prestress the slab. These membrane forces effectively prevent collapse of the bridge, as an almost linearly ascending load-displacement curve

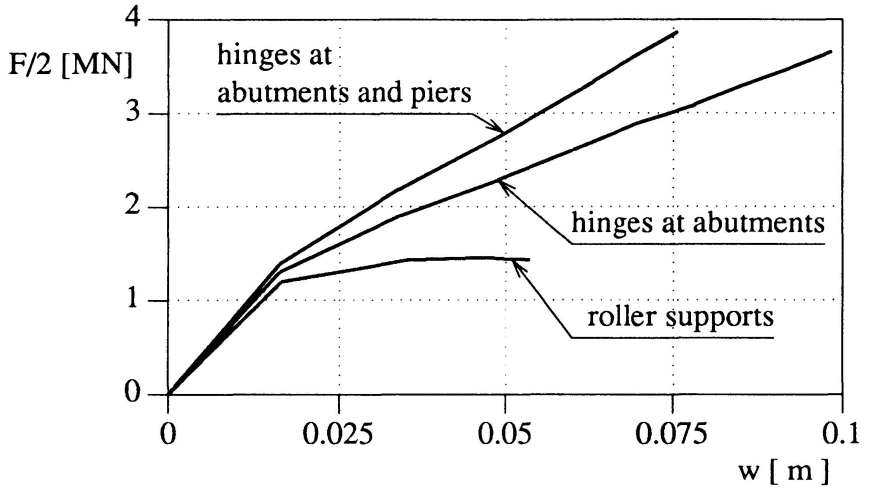

Figure 5 Influence of boundary conditions on load-bearing capacity.

was computed up to a displacement of 0.2 m, at which point the calculations were stopped. At this point a large part of the reinforcement was yielding. Because no real collapse load could be identified at this point, which is far beyond the failure loads predicted by yield line solutions, the role of the membrane forces seems unrealistically high for these boundary conditions.

To further illustrate the important role of the membrane forces an additional analysis was undertaken in which the piers were roller-supported, but where both abutments were modelled as hinges. The membrane actions that develop are now distributed over all three spans and, as a result, the load-displacement curve nicely falls between both extremes. At a deflection of 0.2 m significant yielding of the reinforcement was again observed, but there were no signs of impending collapse.

The solutions with hinges at all supports and with hinges at only one abutment can be considered as upper and lower bound solutions respectively. Because the precise boundary conditions were unknown a more accurate prediction of the collapse load could only be obtained by improving the upper and lower bounds. To this end first the effect of a variation of the hardening modulus of the reinforcement was considered. In particular it was thought that the almost linear rising branch of the analysis with the hinged supports might be caused by the hardening of the reinforcement after first yielding. Therefore analyses were carried out with the same data, but with an ideally-plastic behaviour of the reinforcement. Surprisingly, for both types of boundary conditions the differences were well within 1%.

Next, it was investigated how the type of loading affected the computed load-deflection response. In the actual test the loading was first carried out under load control and when the collapse load was approached a switch was made to displacement control. This could not be simulated in the finite element analyses. As stated most analyses were carried out under arc-length control with equal loads on both loading blocks. Although the precise form of loading should not influence the collapse load the deflections can be affected by a different control scheme. Therefore an analysis was also made under pure displacement control, in which both loading blocks were pushed down by the same amount in each loading step. In this loading arrangement there is no relative tilting of the outermost loading block compared to the other block, which results in a somewhat stiffer response. However, the differences in displacements remained within 10-15% for a given load level.

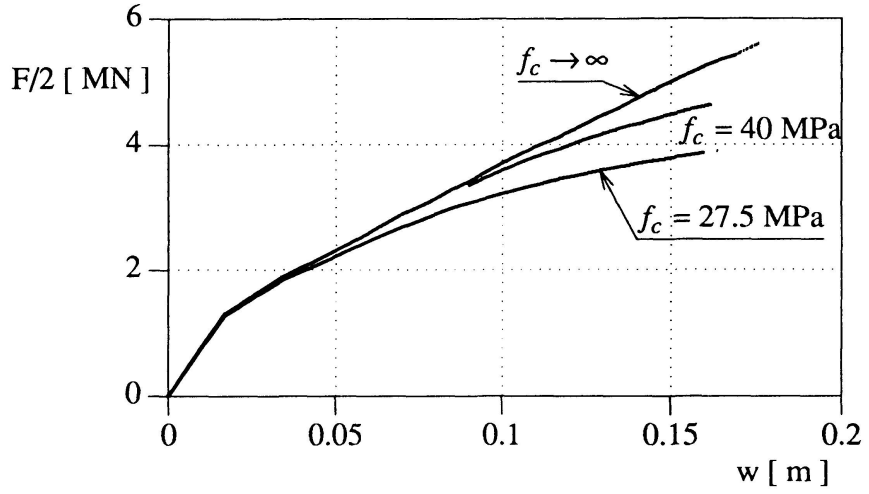

Figure 6 Influence of concrete plasticity on failure load for the case that there are hinges assumed at the abutments and roller supports at all piers.

The most important parameter that influences the upper bound solution is the compressive strength f_c. Figure 6 shows the effect of varying f_c on the load-deflection curves of the upper bound solution. The calculation in which the compressive stresses were not limited, gives the stiffest structural response, but computations with f_c = 40 MPa and f_c = 27.5 MPa give a markedly softer response. In fact, we consider the calculation with f_c = 27.5 MPa as the best upper bound solution, and the structural response should be between this solution and the lower bound solution of Figure 5. It is finally remarked that the lower-bound solution is not affected by adopting a plasticity model to bound the compressive regime, since the maximum compressive stresses remain well below the uniaxial compressive strength f_c.

4. DISCUSSION OF THE RESULTS AND FAILURE MECHANISM

The authors expected that the lower bound solution would be closer to the experiment than the upper bound solution, since it was believed that the abutment was not sufficiently rigid to sustain the large horizontal forces without undergoing horizontal displacements. Accordingly, the most realistic assumption for the conditions at the abutments would be roller supports rather than hinges. This expectation was confirmed when the testing had been carried out, Figure 7.

Although the numerically predicted lower-bound solution for the failure load and the experimentally obtained collapse load agree extremely well, this is not completely the case for the failure mechanism. From observations on the experimental failure pattern it seems that first a pure bending type failure has occurred, but that after significant deformations the shear capacity was exhausted. This point, that is when the capacity to sustain external loads starts to decrease, is marked by the onset of the softening branch in Figure 7. This hypothesis is strengthened by the following observations. Firstly, the used plate/shell elements can only predict accurately bending type failures. Yet, it predicted the experimental failure load very well. Secondly, not only did our (lower-bound) numerical solution, in which membrane effects played no role, match the experimental failure load, also the yield line solutions obtained at the University of Cincinnati [1] fall in the same range, indicating that at the peak of the experimental load-deflection curve only bending effects have played a role of importance. Exhaustion of the shear capacity and subsequent punching only comes into play after significant yielding of the reinforcement.

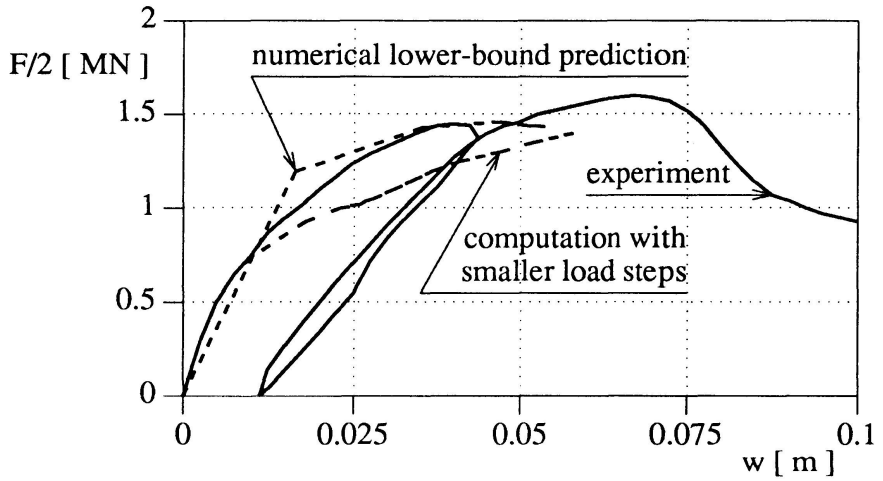

Figure 7 Numerically obtained lower-bound solution and the experimental failure load.

In the numerical simulations yielding started at a load level of $F/2 = 1.05$ MN at the edge of the outermost loading block near the abutment. The extent of the area in which the bottom reinforcement was yielding at a load level of $F/2 = 1.40$ MN is shown in Figure 8. The maximum plastic strains at this point were approximately 0.27%. A recalculation, conducted with smaller load steps, resulted in a somewhat softer response, but the computed failure load was hardly affected, Figure 7.

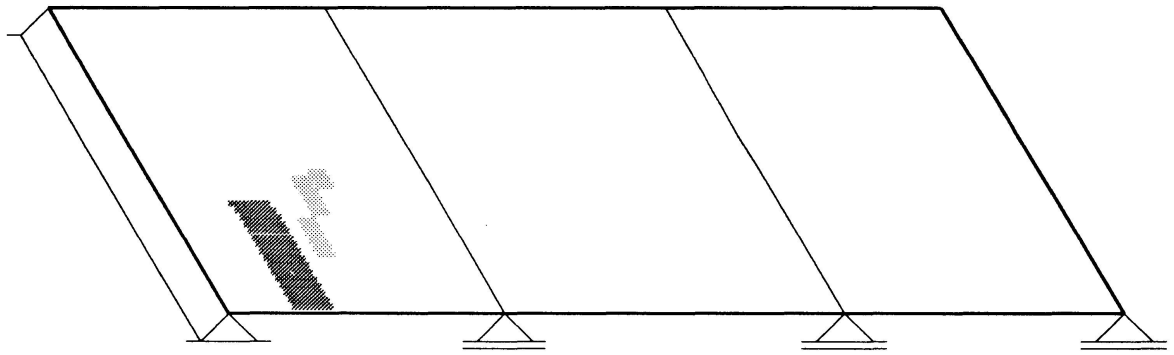

Figure 8 Spread of zone in which the bottom reinforcement is yielding at $F/2 = 1.40$ MN. The lighter shaded area has experienced less plastic flow.

5. CONCLUDING REMARKS

The numerical simulations have shown that the uncertainty in the boundary conditions of the bridge was more important than the fact that the material parameters could not be determined exactly. Nevertheless, reasonable predictions for upper and lower bounds of the failure load could be obtained by a proper combination of sensitivity studies on the influence of the boundary conditions and the material data. The actual field test resulted in a collapse load that was marginally above the predicted numerical lower bound solution.

ACKNOWLEDGEMENTS

Partial financial support from the Commission of the European Communities through the Brite-Euram programme (Project BE-3275) to the first author is gratefully acknowledged.

REFERENCES

1. AKTAN, A.E., MILLER, R. and SHAHROOZ, B., Destructive field testing of a r/c slab bridge and associated analytical correlation studies, Research Status Report, University of Cincinnati, Cincinnati, 1991.

2. BORST, R. de and NAUTA, P., Non-orthogonal cracks in a smeared finite element model, *Engineering Computations* **2** , 1985, pp. 35-46.

3. MEYER, C., Analysis of underwater tunner for internal gas explosion, in *Computational Mechanics of Concrete Structures*, IABSE Reports 54, 1987, pp. 473-486.

4. MIER, J.G.M. van, Examples of non-linear analysis of reinforced concrete structures with DIANA, *Heron* **32** , No. 3, 1987.

5. ROTS, J.G., Computational modeling of concrete fracture, Dissertation, Delft University of Technology, Delft, 1988.

6. SCHELLEKENS, J.C.J., FEENSTRA, P.H. and BORST, R. de, A self-adaptive load estimator based on strain energy, in *Computational Plasticity: Fundamentals and Applications* , Pineridge Press, Swansea, 1992, pp. 187-198.